Adversarial Attack Type I: Cheat Classifiers by Significant Changes

Sanli Tang, Xiaolin Huang, Mingjian Chen, Chengjin Sun, and Jie Yang

Abstract—Despite the great success of deep neural networks, the adversarial attack can cheat some well-trained classifiers by small permutations. In this paper, we propose another type of adversarial attack that can cheat classifiers by significant changes. For example, we can significantly change a face but well-trained neural networks still recognize the adversarial and the original example as the same person. Statistically, the existing adversarial attack increases Type II error and the proposed one aims at Type I error, which are hence named as Type II and Type I adversarial attack, respectively. The two types of attack are equally important but are essentially different, which are intuitively explained and numerically evaluated. To implement the proposed attack, a supervised variation autoencoder is designed and then the classifier is attacked by updating the latent variables using gradient information. Besides, with pre-trained generative models, Type I attack on latent spaces is investigated as well. Experimental results show that our method is practical and effective to generate Type I adversarial examples on large-scale image datasets. Most of these generated examples can pass detectors designed for defending Type II attack and the strengthening strategy is only efficient with a specific type attack, both implying that the underlying reasons for Type I and Type II attack are different.

Index Terms—adversarial attack, type I error, supervised variational autoencoder

I. INTRODUCTION

IN recent years, deep neural networks (DNN) have shown great power on image classification [1], [2], segmentation [3], and generation tasks [4], [5]. But many DNN models have been found to be vulnerable to adversarial examples [6], [7], [8], which prevents deploying DNNs in physical world, e.g., self-driving and surgical robotics. Adversarial attacks reveal inconsistency between the trained DNNs and the oracle, even when they have consensus performance on known examples. This inconsistency shows that DNNs are over-sensitive to adversarial perturbations [9] such that DNNs may incorrectly alter their labels when polluted examples only have slight difference from correctly classified ones. In form, it can be described as the following problem,

$$\begin{aligned} \text{From} \quad x \quad & \text{Generate} \quad x' = \mathcal{A}(x) \\ \text{s.t.} \quad & f_1(x') \neq f_1(x) \\ & f_2(x') = f_2(x) \end{aligned} \tag{1}$$

where f_1 is the classifier to be attacked while f_2 is the attacker, which could be an oracle classifier, e.g., a group of human annotators. In some literature [10], the last requirement, i.e., $f_2(x) = f_2(x')$, is written as $d(g_2(x), g_2(x')) \leq \varepsilon$, which requires the distance of x and x' not exceed a threshold and naturally leads to the same prediction by f_2.

Study on adversarial attack is meaningful to investigate the robustness of DNNs, which is crucial for many applications. For instance, the generated examples, which are generally hard for DNNs, are very valuable for enhancing the neural networks. Moreover, the relationship between the original example x and the adversarial one x', as well as the generating process, is of great importance and may result in insightful understanding for the DNNs. Therefore, since its proposal, adversarial attack, its defense, and its understanding have attracted attention. For example, the fast gradient sign method (FGSM, [6]) can generate adversarial examples in one step via approximately linearizing the classifier. A powerful attack algorithm with a high success rate is designed in [11] by simultaneously minimizing the distortion of the input and the distance between the output of DNNs and the target output.

Without loss of any generality, we can assume that the original sample x has a positive label, i.e., $f_1(x) = f_2(x) = 1$ in (1), and regard the samples in other classes as negative. Then via (1), we generate an example x' such that $f_1(x') = -1, f_2(x') = 1$. In this sense, (1) produces *false negatives* and induces *Type II error*. Study on generating false negatives and preventing Type II error is very important. There has been great progress in the recent years; see, e.g., [6], [7], [10], [12], [13], [14], [15]. However, Type II error is only one side of a coin. Partially emphasizing (1) cannot lead to the ideal: a constant function $f_1(x) = 1, \forall x$ is immune to adversarial attack (1) with ratio of false negatives being zero, but this function is obviously not good. Statistically, Type I error, corresponding to *false positives*, should be simultaneously considered together with Type II error. Their cooperation gives a comprehensive measurement for a classifier: in the extreme case mentioned above, a constant function has no Type II error but has a very high ratio for Type I error, and thus it is not a good classifier.

Adversarial attacks (1), which are to increase Type II error by generating false negatives, have attracted increasing attention recently. But the discussion for Type I error is missing. For

S. Tang, X. Huang, M. Chen, C. Sun, and J. Yang are with Institute of Image Processing and Pattern Recognition and Institute of Medical Robotics, Shanghai Jiao Tong University, Shanghai, P.R. China. (e-mails: {tangsanli, xiaolinhuang, w179261466, sunchengjin, jieyang}@sjtu.edu.cn). S. Tang and X. Huang contributed equally to this work.
Corresponding authors: Jie Yang and Xiaolin Huang.

Type I error, we focus on *false positives*, i.e., from an example x with $f_1(x) = f_2(x) = 1$, we generate an adversarial example x' such that $f_1(x') = 1$ but $f_2(x') = -1$. Mathematically,

$$\begin{aligned} \text{From} \quad x \quad & \text{Generate} \quad x' = \mathcal{A}(x) \\ \text{s.t.} \quad & f_1(x') = f_1(x) \\ & f_2(x') \neq f_2(x). \end{aligned} \quad (2)$$

Adversarial attack relies on inconsistency between the attacked classifier and the attacker. For (1), a small change from x to x' that has no difference in the view of f_2 leads to a sign reversal of f_1. While the new attack (2) shows another inconsistency: f_1 has no response to significant changes happened in f_2. An intuitive example is given in Fig.1, where a classifier trained on MNIST with 98.64% test accuracy is attacked. Starting from a "3" that is correctly identified, i) by (1), we slightly disturb it such that the adversarial digit is still "3" but is identified as "8"; ii) by (2), we really change it to an "8" but f_1 remains as before: the classifier thinks of the adversarial digit as "3".
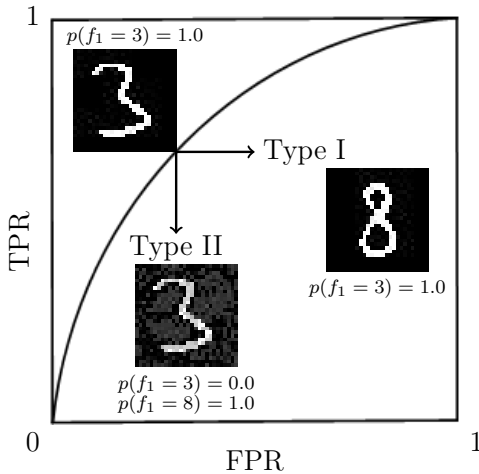

Fig. 1. Relationship between Type I and Type II adversarial attacks on ROC curve of f_1. Through viewing number "3" as true sample and others as false samples, Type II attack aims to decrease the true positive rate (TPR), while Type I attack tries to increase the false positive rate (FPR)

The existing attack (1) and the proposed one (2) aim at Type II and Type I error and thus they are called *adversarial attack Type II* and *adversarial attack Type I*, respectively. They are equally important and irreplaceable. One may argue that Type I and Type II attack can be implemented by each other. For example, one can generate an "8" that is incorrectly identified as "3" from a correct "8" by the existing Type II attack methods, which however requires another example and hence violates (2). The underlying reasons and the corresponding defects of the classifier for Type I and Type II attack are different, which will be detailed in Section II. As a result, many defense methods designed for the existing Type II attack do not work for the proposal Type I attack, which will be shown in Section IV.

Different to Type II attack, where the variant from the original example is quite small, Type I attack requires significant change to transform the true label. Generally, it is more hard since adding noise does not work for Type I attack. In this paper, we design a supervised variational autoencoder (SVAE)

model, which is the supervised extension from original variational autoencoder (VAE) [5]. Based on prior knowledge on Gaussian distribution, embedding label information in the latent space can capture the features. Then on the latent space, we attack the classifier by updating the latent variables by a gradient descent method, which forwards propagates through a decoder to recover the revised latent variables into images. Benefiting from the Gaussian restriction in the latent space and inspired by adversarial autoencoder [16], a discriminator is added to estimate the distribution of the manifold in the latent space and then to successfully implement Type I attack. Note that the Type I attack is not restricted to VAE architecture. Any framework that can transfer the input to a controllable latent space, which means that the samples are expected to follow a known distribution after coding, is possible to conduct Type I attack. In this paper, experiments on AC-GAN [17] and StyleGAN [18] for Type I attack on latent spaces (attack on latent space is designed in [15] for Type II attack) are provided. Other auto-encoder methods and generative models, including [4] [19] [20] [21] [22], are also promising for generating Type I adversarial examples.

The rest of this paper is organized as follows. In Section II, Type I adversarial attack is proposed and its link to Type II attack is discussed. The techniques of Type I adversarial attack are given in Section III. Section IV evaluates the proposed attack on digits and face recognition tasks. The performance under defence designed for Type II attack is also reported, showing essential difference between Type I and Type II attack. In Section V, a conclusion is given to end this paper.

II. TYPE I ATTACK AND ITS RELATIONSHIP TO TYPE II

Deep neural networks have shown powerful fitting capability on training set. Although f_1 and f_2 have very similar performance on known data, they are still different and the inconsistency could be exposed by adversarial attacks. For a training example x, f_1 and f_2 have the same sign, e.g., $f_1(x) = f_2(x) = 1$. The inconsistency happens when x becomes x' in the following two scenarios: i) the attacker f_2 remains the same but the attacked classifier f_1 is oversensitive, i.e., $f_2(x') = 1$ but $f_1(x') = -1$; ii) f_2 has observed the difference but f_1 is over-stable, i.e., $f_2(x') = -1$ but $f_1(x') = 1$.

These two types of adversarial attacks are described by (1) and (2), respectively. Type II attack (1) has been insightfully investigated for attack methods, defense strategies, and theoretical analysis. But Type I attack has not been seriously considered. As summarized in [8], until now, only [23] considers Type I error, however, it is still based on small variations and can be easily discovered. In this paper, we will design a practical Type I attack by designing a supervised variational autoencoder and by gradient updating.

A. Toy Example on Feature Interpretation

Before presenting the detailed technique, we here give a toy example to demonstrate different underlying reasons for Type I and Type II attack in Fig. 2, where yellow circles and green crosses stand for positive and negative training samples.

The data are in a 3-dimensional space and the oracle classifier f_2 uses $x(1)$ and $x(2)$ to distinguish samples. But trained on these samples, f_1 gets 100% accuracy by considering $x(1)$ and $x(3)$. Thus, $x(3)$ is an *unnecessary feature* that is not considered by the oracle but is used in the classifier. Since $x(3)$ is an unnecessary feature, we can shift a true positive along $x(3)$ and the variant cannot be observed by the oracle but makes the result of f_1 change (Type II attack, the blue arrow). The link between unnecessary features and Type II adversarial attack has been theoretically discussed in [10].

To generate another type of adversarial example described in (2), we need to attack *missing features* instead of unnecessary ones. In Fig. 2, $x(2)$ is taken into account in the oracle but is omitted by f_1. Since $x(2)$ is missing, we can change the sample along $x(2)$ until it crosses the decision boundary of f_2 but has no influence on f_1. The change is displayed by the green arrow, by which we successfully generate an example different to x in the view of the oracle but f_1 keeps unchanged. This toy example shows different essence for Type I and Type II attack. To pursue an ideal classifier that can imitate the oracle, it is required to study both unnecessary features by Type II and missing features by Type I attack.
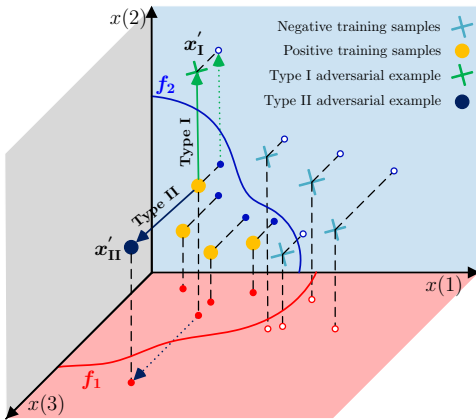

Fig. 2. f_2 is the oracle classifier which uses $x(1)$ and $x(2)$ to distinguish samples shown by green crosses and yellow circles. But trained on these samples, f_1 gets 100% accuracy by considering $x(1)$ and $x(3)$. Here $x(3)$ is an unnecessary feature such that shifting a true positive along $x(3)$ cannot be observed by the oracle but makes the result of f_1 change (Type II attack, the blue arrow). For Type I attack (the green arrow), the sample is moved along $x(2)$ (the missing feature) and an example different to x in the view of the oracle but $f_1(x) = f_1(x')$ is generated.

Real applications are much more complicated than the toy example in Fig. 2, mainly because the features are not strictly orthogonal to each other. But the above feature space interpretation implies that the underlying reasons for Type I and Type II adversarial attacks are different, which follows that the defense methods designed for one type may not work for the other. In numerical experiments, we will show that some defense methods designed for Type II attack do not help the robustness to Type I attack. Worse still, if some method aims at reducing unnecessary features for defending Type II attack, it may make the classifier easier to be attacked by Type I.

Summarizingly, the existing Type II adversarial attack can cheat a classifier by small perturbations that make the classifier have undue change. The proposed Type I adversarial attack cheats a classifier by significant change that is inappropriately ignored by the classifier. The adversarial examples and the generating process for Type II have been found to be interesting and important to analyze neural networks. For most of these topics, Type I attack is indispensable. Take classifier evaluation based on adversarial attacks as an example, where not only Type II error but also Type I error needs to be considered. Another case is classifier strengthening by retraining, for which adversarial examples generated by Type I attack, like $x'_\mathbf{I}$ in Fig. 2, cannot be found by Type II attack. For neural network interpretation, investigating Type II adversarial attack leads to unnecessary features, but missing features can only be captured by Type I attack. Generally, studying adversarial examples from both Type I and Type II attack is helpful.

B. Toy Example on Sphere

To investigate adversarial attacks, an interesting example to classify data from two concentric spheres with different radiuses is designed by [24]. For this simple task, the following single hidden layer network with a quadratic activation function achieves very high accuracy:

$$f_1(x) = w\mathbf{1}\cdot(Wx)^2 + b, \tag{3}$$

where $x \in \mathbb{R}^n$ and $W \in \mathbb{R}^{h \times n}$. According to [24], the above network is equivalent to

$$f_1(x) = \sum_{i=1}^{d} \alpha_i z_i^2 - 1, \tag{4}$$

where z is a rotation of x and d is the rank of W. Based on this equivalence, it was claimed in [24] that adversarial examples could be easily found when $h > n$. Their conclusion is restricted to Type II adversarial examples. In fact, when $h < n$, there still exist Type I adversarial examples. An intuitive explanation is that when $h < n$, $n - h$ dimensions of the input are missed by the classifier such that the values on those dimensions can be arbitrarily modified while keeping the classification result of f_1 unchanged.

Numerically, we consider an experiment that $n = 100, h = 90$ and the samples are uniformly distributed on the concentric spheres with radii being 0.8 and 1.0. Then a network in form (3) is trained through one million steps with 64 batch size, which means 64 million i.i.d. training samples are used in total. After training, 100 thousand random samples are tested and the error rate is less than 10^{-4}, showing that we have already obtained a very good classifier. For the obtained classifier, it is hard to generate a Type II adversarial example, as claimed by [24]. But still, from any sample x with $\|x\|_2 = 0.8$, we can first transform it to z-space, set

$$z'_i = z_i, \forall i = 1, 2, \cdots, 90,$$
$$z'_{91} = z'_{92} = \cdots = z'_{100} = \sqrt{(1 - 0.8^2)/10},$$

and obtain x' from z'. Since the dimension $z_{91}, \ldots, z_{100}$ are missed by f_1, the function value of the generated x' is the same as that of x but x' has been moved to the outer sphere. In practice when the network structure is not clear or the (back) projection is intractable, we can move x to the outer sphere
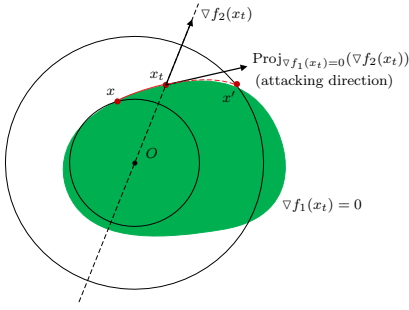
Fig. 3. Illustration of Type I adversarial attack on the sphere dataset [24]. The attacking direction is project of the radial vector onto the surface $\nabla f_1(x_t) = 0$, where x_t is the sample generated at the t-th step.

Fig. 4. The framework for generating Type I adversarial example from the latent space. In this paper, SVAE is proposed for encoding.

by projecting a radial vector onto the surface $\nabla f_1(x) = 0$. The trajectory from x to x' is illustrated in Fig. 3, which also indicates that the basic strategy of Type I adversarial attack we will discuss in the following sections.

III. SUPERVISED VAE MODEL FOR TYPE I ATTACK

Finding an adversarial example to a vulnerable classifier f_1 is substantially an image generation task. Both of the two types of attacks require the generated examples to belong to the wrong classes. But for Type II adversarial attack defined in (1), a violate example x' could be generated by directly manipulating the image space according to the gradients from the $f_1(x)$: typically, $x' = x + \epsilon \nabla_x f_1$, which is the mainstream approach, see, e.g., [6], [25], [26]. The term $\epsilon \nabla_x f_1$ is usually meaningless and could be regarded as inconspicuous noise, which follows that noise detection or de-noising can serve as defenders for Type II attack. Such small disturbance is effective for Type II attack, for which the corresponding adversarial example remains unchanged in the view of the attacker f_2. However, for Type I attack, it is required to generate an adversarial example that is different to the original one in the view of the attacker. Thus, simply considering the gradients in the image space is usually not sufficient. Instead, we need to find a latent space that can capture the features used in both f_1 and f_2. By doing so, we can modify the latent variables and avoid undesirable noise or ghost when reconstructing images from the latent space.

In Fig. 4, we show the designed framework for training the latent space and generating Type I adversarial examples. For the encoder, there are multiple possible paths and in this paper we propose a supervised variational autoencoder (SVAE), i.e., the supervised extension of VAE. For attacking, the gradients from f_1 do not merely propagate to the input x' of f_1 as the traditional methods do, but further to the latent variables z through the decoder. At the same time, the gradients from the attacker are used for revising z to obtain a new image x' with a different label through the decoder. During this process, an equilibrium between f_1 and f_2 is needed to keep the output of f_1 unchanged for achieving the Type I attack.

A. Supervised Variational Autoencoder

Let us first explain the details of SVAE. Based on the generative model of VAE for generating x in the image
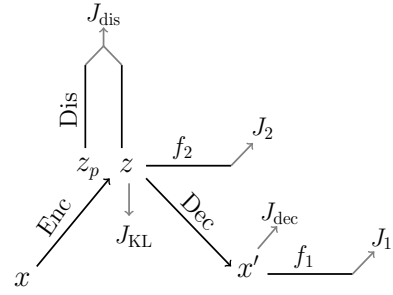
space from latent variables z, which is modeled as $p(x) = \int p(x|z)p(z)dz$, the supervised VAE can be described as $p(x, y) = \int p(x, y|z)p(z)dz$, where y is the label information from the attacker.

Similar to VAE, in order to optimize the supervised variational autoencoder model, we find a lower bound of $p(x, y)$. Assume $q(z)$ is an arbitrary distribution in the latent space, its distance to $p(z|x, y)$ can be measured by Kullback-Leibler (KL) divergence:

$$\begin{aligned} \mathrm{KL}[q(z)\|p(z|x,y)] &= E_{z \sim q}[\log(q(z)) - \log(p(z|x,y))] \\ &= E_{z \sim q}[\log(q(z)) - \log(p(x,y|z)) - \log(p(z))] \\ &\quad + \log(p(x,y)). \end{aligned}$$

The above can be rewritten as:

$$\begin{aligned} &\log(p(x,y)) - \mathrm{KL}[q(z)\|p(z|x,y)] \\ &= -\mathrm{KL}[q(z)\|p(z)] + E_{z \sim q}[\log(p(x,y|z))] \\ &= -\mathrm{KL}[q(z)\|p(z)] + E_{z \sim q}[\log(p(y|z)) + \log(p(x|y,z))]. \end{aligned}$$

The conditional generative methods [16], [27] that use label information as a prior aim to separate the style and content in the latent space. In our setting, latent variables z should contain label information as in [28]. This is mainly due to two reasons: firstly, the distribution in the latent space should be constrained by the attacker according to their labels, which enables the use of gradients from the attacker to modify the generated image; secondly, as described in [10], the judgement of the classifier is decided by a pseudometric measurement in the latent space. Therefore, we replace $p(x|y, z)$ by $p(x|z)$ since z contains the label information y. Then, a lower bound of $p(x, y)$ can be given as:

$$\begin{aligned} \log(p(x,y)) \geq &-\mathrm{KL}[q(z)\|p(z)] + E_{z \sim q}[\log(p(y|z))] \\ &+ E_{z \sim q}[\log(p(x|z))]. \end{aligned} \tag{5}$$

To simplify the optimization, we choose $q(z)$ to be Gaussian depending on x in the latent space, which is also assumed in [5]. Specifically, $q(z|x) = \mathcal{N}(\mu(x; \theta_{\mathrm{enc}}), \sigma(x; \theta_{\mathrm{enc}}))$, from which it follows that SVAE maximizes:

$$\begin{aligned} J = &-\mathrm{KL}[q(z|x)\|p(z)] + E_{z \sim q(z|x)}[\log(p(y|z))] \\ &+ E_{z \sim q(z|x)}[\log(p(x|z))] \\ \triangleq &-(J_{\mathrm{KL}} + J_2 + J_{dec}), \end{aligned} \tag{6}$$

where the three terms are corresponding to the encoder, the classifier, and the decoder in SVAE model, respectively. The

classifier in SVAE imposes a restriction on latent variables to generate images with desired labels through the decoder.

Generally, a classifier trained from data only fits well on the manifold in the latent space of data but might have bad behaviour outside [29]. Since we directly manipulate the latent variables iteratively according to the gradients from the attacker and the attacked classifier, a discriminator is necessary to prevent the latent variables from lying outside the manifold in the latent space while attacking. Consequently, the attacker can provide a stable and effective direction for updating the latent variables under the restraint of the discriminator. In SVAE, the distribution of latent variables is standard Gaussian, which makes a sample-based discriminator applicable. Specifically, a binary discriminator with a sigmoid activation function on the output layer is designed to distinguish the real latent values encoded from input images by the decoder and the fake latent values sampled randomly from Gaussian distribution:

$$J_{\text{dis}} = E_{z_{\text{true}} \sim q(z|x)}[f_{\text{dis}}(z_{\text{true}})] + E_{z_{\text{fake}} \sim \mathcal{N}(0,I)}[1 - f_{\text{dis}}(z_{\text{fake}})]. \tag{7}$$

A two-stage optimization method is utilized in this paper to train SVAE. In the first stage, we simultaneously train the encoder, the decoder, and the classifier to maximize the objective function in (6). The encoder function f_{enc} maps the input x to a Gaussian distribution with its mean and variance to be $\mu(x; \theta_{\text{enc}})$ and $\sigma(x; \theta_{\text{enc}})$. By the reparameterization trick [5], a latent variable z is sampled from such Gaussian distribution, which is then used for classification and recovery as f_2 and f_{dec}, respectively. A gradient descent method Γ, e.g., Adam, is used for training parameters θ_{enc}, θ_2, and θ_{dec}, which are corresponding to f_{enc}, f_2, and f_{dec}.

In the second stage, we train the discriminator f_{dis} to maximize (7) based on the well-located encoder after the first training stage. The input x is first encoded into the Gaussian with mean $\mu(x)$ and variance $\sigma(x)$ in the latent space. Then the positives are sampled from $z_{\text{true}} \sim \mathcal{N}(\mu(x; \theta_{\text{enc}}), \sigma(x; \theta_{\text{enc}}))$, while the negatives are sampled from the standard Gaussian $z_{\text{fake}} \sim \mathcal{N}(0, I)$. A gradient descent method Γ is applied to only update the parameters θ_{dis} in the discriminator f_{dis}. This two stage optimization algorithm is described in Algorithm 1.

Algorithm 1: Two stage learning in SVAE

---
while stage1Training() **do**
  $x, y \leftarrow$ getMiniTrainingBatch()
  $z \sim \mathcal{N}(\mu(x; \theta_{\text{enc}}), \sigma(x; \theta_{\text{enc}}))$
  $(\theta_{\text{enc}}, \theta_{\text{dec}}, \theta_{\text{ora}}) \leftarrow (\theta_{\text{enc}}, \theta_{\text{dec}}, \theta_{\text{ora}})$
      $+\Gamma(\frac{\partial J}{\partial \theta_{\text{enc}}}, \frac{\partial J}{\partial \theta_{\text{dec}}}, \frac{\partial J}{\partial \theta_{\text{ora}}})$
end while
while stage2Traning() **do**
  $x, y \leftarrow$ getMiniTrainingBatch()
  $z_{\text{true}} \sim \mathcal{N}(\mu(x; \theta_{\text{enc}}), \sigma(x; \theta_{\text{enc}}))$
  $z_{\text{fake}} \sim \mathcal{N}(0, I)$
  $\theta_{\text{dis}} \leftarrow \theta_{\text{dis}} + \Gamma(\frac{\partial J_{\text{dis}}}{\partial \theta_{\text{dis}}})$
end while

B. Image Transition Task

Based on the trained SVAE, we are going to generate a Type I adversarial example x' from an original example x as described in (2) such that x' and x have different labels in the view of f_2 but are recognized as the same class by f_1. The first and an easier step is to transform the input image x into another image x' with a different label, which is an image transition task. In our framework, the class information is not directly given, e.g., in the conditional generation methods, but comes from the supervised term in the attacker. The latent variables are revised iteratively according to the gradients from the f_2 and recovered into images through the decoder. Specifically, the objective function for generating targeted examples is:

$$\begin{aligned} J_{\text{IT}} &= J_2(z, y') + \alpha(1 - f_{\text{dis}}(z)) + \gamma ||z||_2 \\ &= -y' \text{log} f_2(z) + \alpha(1 - f_{\text{dis}}(z)) + \gamma ||z||_2, \end{aligned}$$
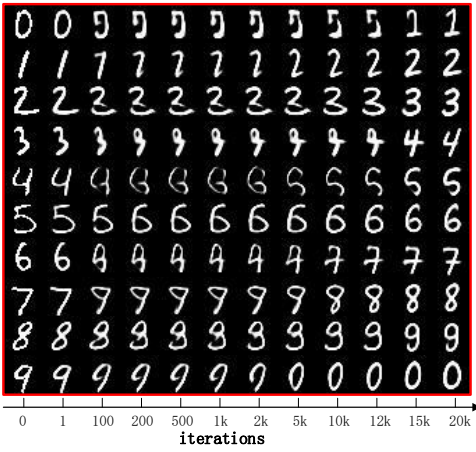
where the cross-entropy loss is applied to f_2 and it is a common choice in classification tasks [1], [2]. Besides, a loss term with the weight α from discriminator f_{dis} is also added in order to prevent z from moving outside of the manifold in the latent space. An l_2 regularization term on z with the weight γ is used to restrict z to locate in the standard Gaussian space as the ambient space of the manifold.

Here, we utilize the established method for image transition for digit images from MNIST and face images from CelebA. For MNIST dataset, a classifier with 98.64% test accuracy is established and then used to image transition: from an image "i" to generate "$i + 1$". For CelebA, a gender classifier with 94.9% test accuracy is established and used to change an image's gender. The transition performance is illustrated in Fig. 5, where the left column represents the original image, the right column shows the generated image with a desired label, and the middle ones are transitory images in different iterations.
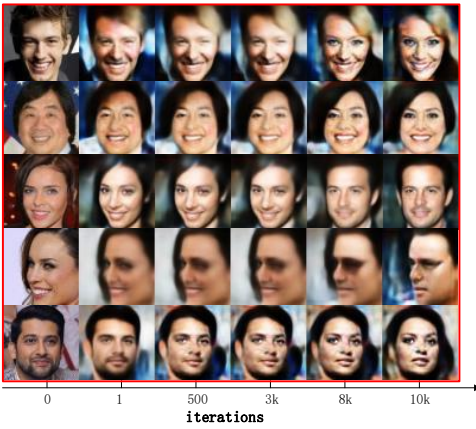
Note that the image transition task is different to feature transformation, for which the typical route is to establish semantic features and change the required one; see, e.g., Fader Networks [30] and Deep Feature Interpolation [31]. The image transition here is implemented under the guide of the classifier f_2. For visuality, we choose f_2 to be a gender classifier, but it is not necessary to have semantic meaning and could be comprehensive. The difference could also be visually observed: the face generated by Fader Networks looks very similar to the original one, since the features have been decoupled; while in Fig.5(b), the generated and the original one could be regarded as different persons.

C. Generating Adversarial Examples for Type I Attack

In the above image transition task, we successfully generate new examples with desired labels. Further, incorporating the attacked classifier f_1 as illustrated in Fig. 4, we try to keep the output of f_1 unchanged, i.e., to generate Type I adversarial examples as described in (2). For a classifier f_1, an adversarial example x' with the target label y' of an input x with the original label y is generated through minimizing the following function, where the trained SVAE model is the attacker,

(a)

(b)

Fig. 5. Illustration of supervised image class transition by SVAE on (a) MNIST and (b) CelebA datasets. The target class for digital image i is $i+1$ (the target of "9" is "0") and for male/female face images is the opposites.

$$J_{\text{SA}} = J_{\text{IT}} + k_t J_1(x', y, \cdot)$$
$$= -y' \log f_2(z) + \alpha(1 - f_{\text{dis}}(z)) + k_t J_1(f_{\text{dec}}(z), y, \cdot)$$
$$+ \gamma \|z\|_2. \tag{8}$$

Here, $J_1(x', \cdot)$ is the loss function of the attacked classifier and may take different formulations for different tasks. In multi-class classification tasks, e.g., [1], [2], $f_1(x)$ is a vector of probabilities for each class. While in face recognition tasks [32], $f_1(x)$ is a feature vector, where a small distance $\|f_1(x') - f_1(x)\|_2$ means that x and x' tend to be the same person. For these two tasks, the $J_1(x', \cdot)$ could be set as the following,

$$J_1(x', \cdot) = \begin{cases} -y \log f_1(x') & \text{classification tasks,} \\ \|f_1(x') - f_1(x)\|_2 & \text{face recognition tasks.} \end{cases} \tag{9}$$

In (8), there is a positive parameter k_t reflecting the stress we put to keep the attacked classifier f_1 unchanged. In our method, k_t could vary for different iterations. Generally, at the beginning, we allow variation on the output of f_1 to really change the image. Later, k_t increases to pull the image back such that the output of f_1 is as the same as the original.

Specifically, a self-adaptive weight strategy is designed for k_t to maintain such equilibrium:

$$k_{t+1} = k_t + \eta \left(\beta J_1(f_{\text{dec}}(z), y, \cdot) - J_2(z, y') \right.$$
$$\left. + \max \left\{ J_1(f_{\text{dec}}(z), y, \cdot) - \hat{J}_1, 0 \right\} \right). \tag{10}$$

In our experiments, after increasing the equilibrium weight in several iterations, k_t is clipped into $[0, 0.001]$. The hyperparameter β, inspired by [33] to control the equilibrium between the losses J_1 and J_2, is set as

$$\beta = \frac{J_2(z, y')}{J_1(x', y, \cdot)} = \frac{J_2(z, y')}{J_1(f_{\text{dec}}(z), y, \cdot)}. \tag{11}$$

A lower β means that the generated adversarial sample x' more likely belong to the targeted label y' yet the probability of f_2 judging that $f_2(x) \neq f_2(x')$ is higher. In (10), an additional term $\hat{J}_1$ is used as the target value for the attacked classifier. It is introduced in a hinge loss term to sacrifice a little confidence properly in f_1 to concentrate more on f_2 which makes the input image really become a new image with different classes. This term can improve the image quality and success rate for Type I attack.

We update the latent variable z iteratively to minimize the objective function in (8) after all those networks are well trained. At the start, we initialize z to be the mean of the Gaussian $z_{\text{init}} = \mu(f_{\text{enc}}(x))$ according to the given input x. Similar to training networks, we here use Adam [34] to optimize (8) on the latent variable z iteratively. The overall algorithm for generating Type I adversarial examples is illustrated in Algorithm 2. Obviously, 0 is a lower bound of J_{SA} in both classification and recognition tasks. Therefore, the convergence is guaranteed when optimizing J_{SA} through the gradient descent methods. Codes are provided in supplemental materials (SM) and will be published in the future.

Algorithm 2: Generating Type I Adversarial Attack

given input x
$z_0 \leftarrow \mu(x; \theta_{\text{enc}})$, $k_0 \leftarrow 0$, $t \leftarrow 0$
while not converging() **do** $\quad z_{t+1} \leftarrow z_t + \Gamma(\frac{\partial J_{\text{SA}}}{\partial z})$
$\quad x'_{t+1} \leftarrow f_{\text{dec}}(z_{t+1})$
$\quad k_{t+1} \leftarrow k_t + \eta(\beta J_1(x'_{t+1}, y, \cdot) - J_2(z, y') +$
$\quad\quad\quad \max\{J_1(f_{\text{dec}}(z), y, \cdot) - \hat{J}_1, 0\})$
$\quad k_{t+1} \leftarrow \max\{0, \min\{k_{t+1}, 0.005\}\}$
end while
$x' = f_{\text{enc}}(z_T)$, T is the final time step
return x'.

D. Attack on Latent Space

The adversarial attacks reveal weaknesses of neural networks and provide tools to analyze neural networks. Although most of the existing attacks are for image input, the attacks may happen on non-image data. Recently, an interesting attack on the latent space is designed by [15]. Suppose z is an original vector in the latent space and that attack is to generate z' such that $\|z - z'\|$ is small but via a generative model, e.g., AC-GAN [17] is used in [15], the generated images $G(z)$ and $G(z')$ are

incorrectly identified by the attacked classifier f_1 into different classes, i.e., $f_1(G(z)) \neq f_1(G(z'))$. The original z could be either given or randomly generated. This kind of attacks get rid of the encoder and are applicable for non-image data.

From the above description, one could observe that the attack designed in [15] belongs to Type II attack. Parallelly, we could also design Type I attack on latent space, which is mathematically described as the following problem,

$$\begin{aligned} \text{From} \quad z \quad &\text{Generate} \quad z' = \mathcal{A}(z) \\ \text{s.t.} \quad &f_1(G(z')) = f_1(G(z)), \quad (12)\\ &\|z - z'\|_2^2 \geq \varepsilon \end{aligned}$$

where f_1 is the attacked classifier, G is a generative model, and ε is a user-defined threshold. Actually, (12) is a special case of (2), where we use a naïve distance-based classifier as the attacker. Basically, along a direction in the manifold where $f_1(G(z))$ keeps a constant, we can go away from z and find Type I adversarial examples on the latent space. Specifically, those adversarial examples could be generated by minimizing the following loss function,

$$L(z') = kJ_1(G(z'), \cdot) + \max\left\{\varepsilon - \|z' - z\|_2^2, 0\right\}, \quad (13)$$

where J_1 is defined as (9), G is a generative model that has been trained in advance, and k is a trade-off parameter. The first term in (13) forces f_1 to judge the two generated samples $G(z')$ and $G(z)$ to be the same class, while the second term encourages z' to leave the original z. A smaller k means we allow a larger change on f_1 in order to obtain a larger distance in the latent space. We could design a self-adaptive strategy as (10) for k but in this paper, we keep k unchanged during the whole process. If an auxiliary classifier is modeled in G, like AC-GAN [17] and is denoted by f_G, then we could also minimize the difference of $f_G(z')$ and y_{target} to assign a target label, otherwise, the attack is untargeted.

IV. EXPERIMENTAL VALIDATION

In this section, we validate the proposed method for this new type of adversarial attack. There are two main questions: i) whether the proposed method can change an image significantly but keep the attacked classifier unchanged; ii) whether there is essential difference from the existing adversarial attack. For the two purposes, we first validate the proposed attack on MNIST dataset [35], where new generated digits will be recognized as the original ones, and on CelebA dataset [36], where new face images with different genders are generated but will be identified as the same person. After that, we apply defense methods to defend attacks. The different performance of Type I and Type II attack confirms their essential difference. At last, Type I attacks on latent space are evaluated, which also shows the possibility of using different generative models for Type I attack.

For SVAE training, we use Adam [34] with learning rate 0.0002. The hyper parameters α and γ in (8) are set to be 0.01 and 0.0001, respectively. β for equilibrium in (10) is 0.001. During the attacking iterations, Adam is utilized to update latent variable z with learning rate 0.005. The target loss $\hat{J}_1$ in (10) is set to 0.01 as the cross entropy loss for the digital
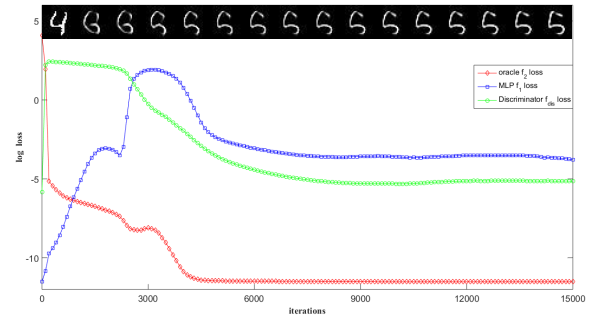

Fig. 6. Illustration of the log loss terms of the attacker f_2, the discriminator f_{dis} and the MLP f_1 by setting $y' = 5$ and $y = 4$ in (8). The lower loss of f_1, the more it is believe the generated image belongs to class "4". Until convergence, f_1 still classifies it as "4" with 99.41% confidence.

image classification task and 1.00 as the Euclidean distance for the face recognition task. The detail of SVAE's architectures is provided in the SM. For datasets, MNIST contains 60K handwritten digital images of size 28x28. Following the common split, we use 50K images for training and rest for test. CelebA dataset includes more than 200K face images with 40 attribute annotations. We simply split CelebA dataset into Male/Female subsets according to their gender labels, which are then normalized and centrally cropped into size 64x64. All the experiments in this paper are implemented in Tensorflow [37] on an NVIDIA TITAN X GPU with 12GB memory.

A. Type I Attack on Digits Classifier

First we use the proposed method to attack a classifier trained on MNIST dataset. The attacked classifier f_1 is an MLP with 128 hidden units and achieves 2.73% test error. We train an SVAE model, which has 1.36% test error and serves as the attacker f_2. Then from a given image that has been correctly classified by f_1, we apply Algorithm 2 to generate an adversarial example. The target is to change an "i" to an "$i + 1$" that is still wrongly classified as "i" by f_1.

In Fig. 6, we illustrate the log loss terms of the attacker f_2, the discriminator f_{dis}, and the MLP f_1, when SVAE tries to conduct a Type I attack to transform an image from "4" to "5" while the MLP still classifies it as "4". The images on the top are the generated adversarial examples x' at the corresponding iterations. Notice that the loss for f_2 is relative to $y' = 5$ while the loss for f_1 is with respect to $y = 4$. Therefore, at the beginning, the loss of f_2 is much higher than that of f_1 due to the fact that the original image is the number "4". Then, through minimizing J_{SA} in (8), the image is gradually converted to number "5" while the loss of f_1 is increasing, since the target loss $\hat{J}_1$ is set to 0.01 and the weight for J_1 in (10) is clipped into 0. At the same time, the loss of the discriminator is increasing since the latent variables have to walk beyond the manifold in the latent space. When J_1 increases beyond $\hat{J}_1$ and J_2 is lower than the equilibrium described in (11), the adaptive weight k_t for J_1 increases to pull down J_1 until convergence. Although the loss of the attacker f_2 decreases rapidly at the beginning, the supervised information from the attacker is not very reliable since its performance is unpredictable outside the manifold

in the latent space. The discriminator, therefore, plays a key role in restraining the latent variables into the manifold, which makes the classifier in SVAE to provide convincible gradients.

In Fig. 7(a), we show some examples of Type I attack on the digit classifier. The original images are plotted in the left column, the generated ones are in the right column, and the gradually changing process is shown between them. The number marked on the top of each image indicates the confidence of being the original class given by the attacked classifier f_1. During the attack, the confidence will first drop and then increase, which coincides with our setting of k in Algorithm 2, as discussed in Section III.C.

B. Type I Attack on Face Recognizer

Next, we evaluate the proposed attack on a face recognizer FaceNet [32]. We directly use the FaceNet trained on CelebA, which achieves 99.05% accuracy on LFW [38] dataset for face recognition. The same face alignment, whitening, and other pre-processing procedures are carried out as recommended [32] in our experiment. An SVAE is trained on CelebA dataset with a gender classification f_2 of 94.9% accuracy. Our task is to transform the gender of an image but keep it recognized as the same person by the FaceNet. There is an interesting difference between this task and the previous one. In the previous task, the attacker is stronger than the attacked classifier. But for this task, the SVAE classification accuracy is lower than the attacked FaceNet. Moreover, being the same gender is a necessary condition of the same person and the network of FaceNet is much deeper and more complicated. Even in the case that f_1 is stronger than f_2, the proposed Type I attack could succeed.
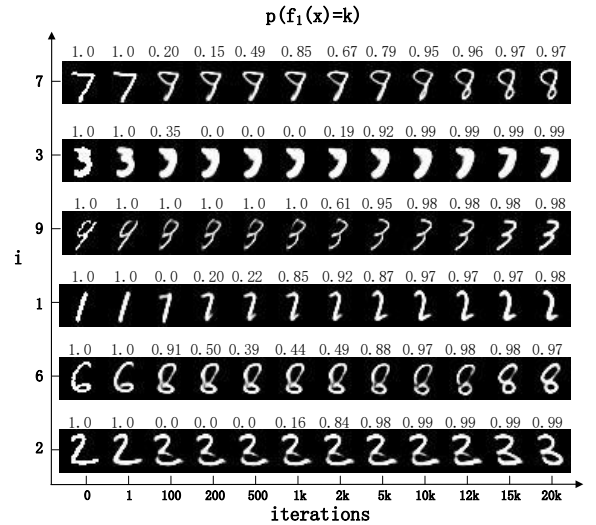
Some typical adversarial examples are given in Fig. 7 (b). For each pair, the left face is in CelebA and the right one is generated by Algorithm 2. The number above the images are the distances given by the FaceNet, for which the threshold of being the same person is suggested to be 1.242 by [32].

To evaluate the success rate of Type I attack, we generate adversarial examples from the first 1000 images of the validation set in CelebA. When saying that the attack is successful, we mean the image pair (x, x') satisfies three conditions: i) $f_1(x) = f_1(x')$, i.e., the two faces are recognized as the same person by the FaceNet; ii) $f_2(x) \neq f_2(x')$, i.e., they are of different genders in the view of f_2 and are not the same person; iii) x' is indeed a face. The latter two criteria are judged by thirty annotators and the average successful rate is 69.8%. All the generated faces are provided in SM for reference.
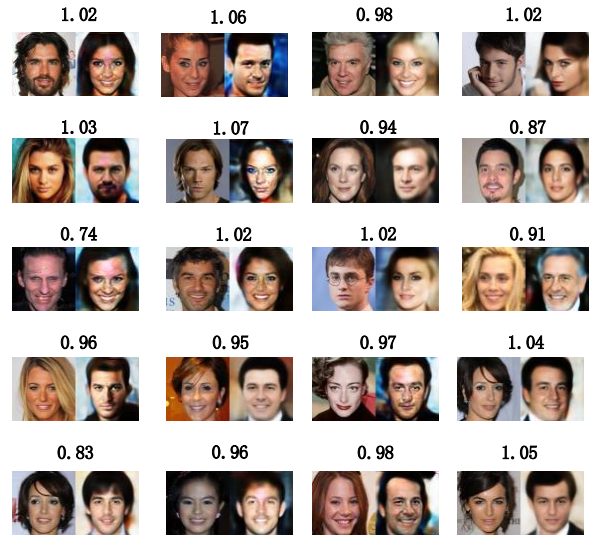
C. Type I Attack Defenses by Detecting

The above two experiments validate the effectiveness of generating Type I adversarial examples. As previously discussed, Type II attack reflects the over-sensitivity and the Type I attack relies on the over-stability of the classifier. Since the underlying reasons are different, we expect that defense strategies designed for Type II attack by detecting the adversarial input do not help much for Type I attack.

To validate this corollary, we use the proposed method to attack the MLP with a feature squeezing defense strategy [39]

(a)

(b)

Fig. 7. (a) Adversarial examples with the probabilities according to iteration steps on MNIST dataset. (b) Adversarial example pairs with Euclidean distance on the top measured by FaceNet. Note that 1.242 is the distance threshold adopted by FaceNet to judge whether two images are from the same person.

that is the most effective defense strategy and has shown great potential to counter many existing Type II attacks. The feature squeezing defense strategy is to detect adversarial examples by reducing the degree of input features available to adversarial examples. Specifically, it calculates the distance between the classifiers' prediction (e.g., the output of the softmax layer) of the input sample and its squeezing one. If the distance is larger than a given threshold, the defense method regards the input sample as an adversarial example and refuses to classify this sample. The defense strategy can be summarized as bellow:

$$\widetilde{f}_1(x) = \begin{cases} f_1(x), & D(f_1(x), f_1(F(x))) < \zeta, \\ \text{reject}, & \text{otherwise}, \end{cases}$$

where $F(x)$ is the feature squeezing strategy, $D(\cdot, \cdot)$ is a distance metric, and ζ is the hyper-parameter serving as a

threshold to judge whether the input x is an adversarial example (then reject it) or not. Following the common setting in [39], the joint squeezers with one bit depth reduction and a 2×2 median smoothing are set for the feature squeezing strategy F, which presents the highest detection rate as revealed in [39]. The distance metric D is chosen to be Euclidean distance. We randomly choose 500 samples on MNIST test set and calculate the detection rate on clean test samples, their Type I adversarial examples, and their Type II adversarial examples with different thresholds. Type I and Type II adversarial examples are generated by Algorithm 2 (SVAE), FGSM [6], DeepFool [25], CW [12], and EAD [13], respectively. The detection rates, i.e., the rate of being recognized as adversarial examples by the detector, for the clean samples, Type I adversarial examples, and Type II adversarial examples are listed in Table I. For different ζ values, the detection rates for clean and Type I adversarial examples have no significant difference, which means that Type I adversarial examples cannot be well distinguished from clean data. By contrast, the detection ratio for Type II adversarial examples is significantly higher than that for clean data, showing that feature squeezing is a good detection method for Type II attack, but does not work for Type I attack.

TABLE I
DETECTION RATES ON MNIST TEST SET, TYPE I ADVERSARIAL EXAMPLES AND TYPE II ADVERSARIAL EXAMPLES WITH DIFFERENT THRESHOLDS.

	ζ	0.2510	0.6089	0.9353
	Clean	0.234	0.102	0.050
Type II	FGSM [6]	0.870	0.776	0.726
	DeepFool [25]	0.998	0.974	0.872
	CW$\_l_2$ [12]	0.998	0.976	0.842
	EAD [13]	0.998	0.980	0.902
Type I	SVAE	0.306	0.122	0.076

Similar phenomenon on the feature squeezing could also be observed in attacking FaceNet, for which 1000 Type I adversarial examples are generated as described in Section IV.B. The same number of Type II adversarial examples are generated by the projected gradient descent (PGD, [14]). We set $\zeta = 1.2$ and consider different sizes of the smoothing kernel. The detection rates can be found in Table II, showing that feature squeezing does not help for Type I attack since Type I attack is not built on adding noise.

TABLE II
DETECTION RATES ON CELEBA TEST SET THROUGH THE FEATURE SQUEEZING DEFENSE METHOD.

Filter size	Clean	Type I (SVAE)	Type II (PGD)
3×3	0.000	0.000	0.487
5×5	0.064	0.032	0.971

D. Type I Attack Defenses by Strengthening

Feeding back the adversarial examples to re-train the classifier is another method to increase the robustness of networks.

In the following, we use MNIST dataset to test the defending performance of Adversarial Logit Pairing [40], which is designed for Type II adversarial examples. The attacked classifier is LeNet [41]. After strengthening, adversarial examples generated by attacking the original networks are used for validation. The accuracy for Type II attack is improved to 98.5%, since minimizing the pairwise logit pairing loss $L(f(x), f(x'))$ that requires a small distance between the original example x and the adversarial one x' is helpful. However, this setting does not work for Type I attack: if x' is generated by Type I attack, then x and x' do not belong to the same class and $L(f(x), f(x'))$ is not expected to be small. In our experiment, the accuracy for Type I attack is only 14.2%, verifying that the logit pairing technique cannot be directly used for the Type I adversarial examples.

As suggested and numerically verified by [42], adding adversarial examples generated from other attacks is helpful, which is based on the transferability across different models and attack methods. An interesting question is that whether the capability of defending one type of adversarial attack could help against another type. To answer this question, we strengthen FaceNet by Type I, Type II (FGSM), and Type II (PGD) adversarial examples, respectively. For Type II attack, we use the adversarial logit pairing method. For Type I attack, the adversarial logit pairing does not help as shown before, so we turn to vanilla adversarial training. Specifically, adversarial examples generated by attacking the original networks are randomly split into two parts with equal probability. One subset is sent back together with LFW dataset for adversarial training. Then strengthened FaceNets are evaluated on the rest adversarial examples. The classification accuracy could be found in Table III. The diagonal shows the performance of defending the adversarial attack by adversarial training on the same attack method. Other elements show the transferability of adversarial training. One could find that strengthening FaceNet by FGSM can improve the robustness against PGD; and vice versa. However, strengthening by Type II adversarial examples has little effect on defending Type I attack, showing their difference.

TABLE III
CLASSIFICATION ACCURACY OF FACENET STRENGTHENED BY DIFFERENT ATTACK METHODS ON ADVERSARIAL EXAMPLES

strengthened	LFW	Type I (SVAE)	Type II (FGSM)	Type II (PGD)
by SVAE	0.990	0.554	0.987	0.998
by FGSM	0.995	0.110	1.000	0.996
by PGD	0.997	0.140	0.998	1.000

E. Type I Attack on Latent Space

In the last experiment, we will consider Type I attack on latent spaces. Attacks could happen on non-image data. But to visualize the performance, we apply a generative model to transfer a latent vector to an image. The attack design is independent of the generative model. For attacking LeNet [41] on MNIST, we choose AC-GAN [17], which is also used in [15]. For attacking FaceNet on CelebA [36], we use StyleGAN

[18], which is one of the state-of-the-art generative models. We train an AC-GAN with 128 latent features on MNIST and use StyleGAN with 512 latent features provided by [18]. Since these generative models only affect the visual quality but have no difference on attack performance, we do not report their structures and training details here. Based on trained generative models, we attack the classifier f_1 by minimizing (13), where the hyper-parameters are set as $k = 10^{-2}, \varepsilon = 0.1$ for attacking LeNet, and $k = 10^{-3}, \varepsilon = 0.35$ for attacking FaceNet, respectively. Adam with the learning rate 0.01 is used.

In Fig. 8, Type I attack on latent space is displayed by plotting the generative images (in 28×28) by AC-GAN. Each pair of those digits are visually different, however, they are identified to the same class by the attacked LeNet. Since AC-GAN has an auxiliary classifier, we can utilize this classifier to set a target label.

Fig. 8. Type I attack performance on the latent space of AC-GAN. For each pair of the digits, the attacked LeNet correctly recognizes the left digit but incorrectly thinks the right one belongs to the same class.

In Fig. 9, we display 6 face sequences generated by the Type I adversarial attack on the latent space of StyleGAN. Thanks to the great generative ability of StyleGAN, the adversarial images are in the size of 1024x1024. Starting from the left face in each row, the attack significantly changes the appearance. However, the attacked FaceNet still recognizes them as the same person. Differently to the attack shown in Fig.7(b), the attack based on StyleGAN can not control the change direction, e.g., from male to female or the opposite. In the future, it is of great interest to implement targeted Type I attack based on StyleGAN or other generative models.

V. CONCLUSION

False positive and false negative rates are important evaluation criteria for the performance of classifiers, thus, adversarial attacks aiming at false positivists (Type I attack, proposed in this paper) and at false negatives (Type II attack, the current popular ones) are both deserved to be investigated. The inconsistency in the feature spaces makes classifiers vulnerable. But the underlying reasons for Type I and Type II attack are different: Type I attack relies on the missing features that are utilized by the attacker but are ignored by the attacked classifier, while Type II attack modifies the unnecessary features that are meaningless for the attacker but are concerned by the attacked classifier.

To generate false positives is to cheat a classifier by significant changes. The generative target is a totally new sample that is misclassified into the same class of the original by the
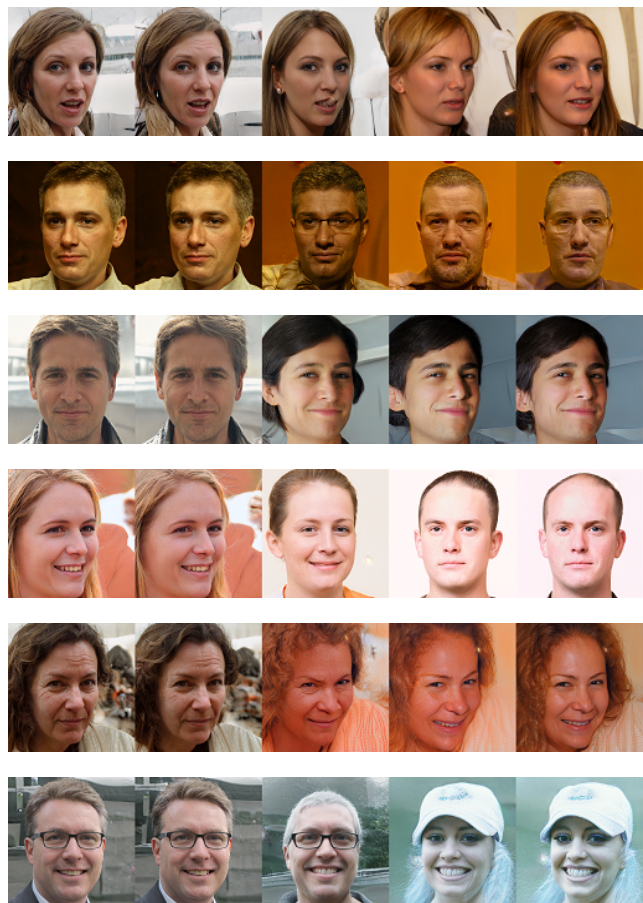

Fig. 9. Type I attack on the latent variables of StyleGAN. The left column shows the generated faces corresponding to the starting latent variable, the right column shows the attack results, and the intermediate images are displayed in the middle. The image size is 1024×1024. For all the 6 rows, the distances judged by FaceNet between the left and the right are: 0.6780, 0.6321, 0.7632, 1.0482, 0.6448, and 1.0449 (from top to bottom), which are all below 1.242. Though the appearances have been changed significantly, the faces in each row are still identified as a same person by FaceNet.

attacked classifier. For Type I adversarial attack, a supervised variational auto-encoder framework is designed as a generative method. In this framework, the attacker is modeled explicitly to provide supervised information for generating a new and meaningful adversarial example. Rather than directly manipulating in the image space which leads to noise eventually, a generating algorithm for Type I attack is then established by revising the latent variables in the latent space according to the gradients from both the attacker and the attacked classifier, and then those updated variables are recovered into images through a decoder. In order to obtain stable and convincible gradients from the attacker, a discriminator is designed to restrict latent variables to locate on the manifold through the iterative generating algorithm.

In numerical experiments, the proposed method successfully generates Type I adversarial examples to cheat well trained classifiers. Most of these examples can pass feature squeezing detection, an efficient detection method for Type II attack, implying the different essential reasons for Type I and Type II attack. Because of the difference, the current strengthening methods do not have type-crosses capability, i.e., retraining

neural networks by Type II adversarial examples have no benefits on defending Type I attack. Generally, Type I adversarial attack is a new adversarial attack and is of great importance for understanding neural networks. The proposed method is only one way to generate Type I adversarial examples and other architectures with auto-encoder and generative capability are also promising for Type I attack, which can be used for classifier evaluation, classifier re-training, and feature analysis.

ACKNOWLEDGMENT

REFERENCES

[1] K. He, X. Zhang, S. Ren, and J. Sun, "Deep residual learning for image recognition," in *Proceedings of the IEEE conference on computer vision and pattern recognition*, 2016, pp. 770–778.

[2] A. Krizhevsky, I. Sutskever, and G. E. Hinton, "Imagenet classification with deep convolutional neural networks," in *Advances in Neural Information Processing Systems*, 2012, pp. 1097–1105.

[3] H. Zhao, J. Shi, X. Qi, X. Wang, and J. Jia, "Pyramid scene parsing network," in *IEEE Conference on Computer Vision and Pattern Recognition*, 2017, pp. 2881–2890.

[4] I. Goodfellow, J. Pouget-Abadie, M. Mirza, B. Xu, D. Warde-Farley, S. Ozair, A. Courville, and Y. Bengio, "Generative adversarial nets," in *Advances in Neural Information Processing Systems*, 2014, pp. 2672–2680.

[5] D. P. Kingma and M. Welling, "Auto-encoding variational Bayes," *arXiv preprint arXiv:1312.6114*, 2013.

[6] I. J. Goodfellow, J. Shlens, and C. Szegedy, "Explaining and harnessing adversarial examples," *arXiv preprint arXiv:1412.6572*, 2014.

[7] G. Katz, C. Barrett, D. L. Dill, K. Julian, and M. J. Kochenderfer, "Towards proving the adversarial robustness of deep neural networks," *arXiv preprint arXiv:1709.02802*, 2017.

[8] X. Yuan, P. He, Q. Zhu, R. R. Bhat, and X. Li, "Adversarial examples: Attacks and defenses for deep learning," *arXiv preprint arXiv:1712.07107*, 2017.

[9] C. Szegedy, W. Zaremba, I. Sutskever, J. Bruna, D. Erhan, I. Goodfellow, and R. Fergus, "Intriguing properties of neural networks," *Computer Science*, 2013.

[10] B. Wang, J. Gao, and Y. Qi, "A theoretical framework for robustness of (deep) classifiers against adversarial examples," *arXiv preprint arXiv:1612.00334*, 2016.

[11] N. Papernot, P. Mcdaniel, X. Wu, S. Jha, and A. Swami, "Distillation as a defense to adversarial perturbations against deep neural networks," in *Security and Privacy*, 2016, pp. 582–597.

[12] N. Carlini and D. Wagner, "Towards evaluating the robustness of neural networks," in *Security and Privacy*, 2017, pp. 39–57.

[13] P. Y. Chen, Y. Sharma, H. Zhang, J. Yi, and C. J. Hsieh, "EAD: Elastic-net attacks to deep neural networks via adversarial examples," *arXiv preprint arXiv:1709.04114*, 2017.

[14] A. Madry, A. Makelov, L. Schmidt, D. Tsipras, and A. Vladu, "Towards deep learning models resistant to adversarial attacks," *International Conference on Learning Representations*, 2018.

[15] Y. Song, R. Shu, N. Kushman, and S. Ermon, "Constructing unrestricted adversarial examples with generative models," *Neural Information Processing Systems*, pp. 8312–8323, 2018.

[16] A. Makhzani, J. Shlens, N. Jaitly, I. Goodfellow, and B. Frey, "Adversarial autoencoders," *arXiv preprint arXiv:1511.05644*, 2015.

[17] A. Odena, C. Olah, and J. Shlens, "Conditional image synthesis with auxiliary classifier GANs," *International Conference on Machine Learning*, pp. 2642–2651, 2017.

[18] T. Karras, S. Laine, and T. Aila, "A style-based generator architecture for generative adversarial networks." *arXiv: Neural and Evolutionary Computing*, 2018.

[19] S. Baluja and I. Fischer, "Adversarial transformation networks: Learning to generate adversarial examples," *arXiv preprint arXiv:1703.09387*, 2017.

[20] H. Lee, S. Han, and J. Lee, "Generative adversarial trainer: Defense to adversarial perturbations with GAN," *arXiv preprint arXiv:1705.03387*, 2017.

[21] C. Xiao, B. Li, J.-Y. Zhu, W. He, M. Liu, and D. Song, "Generating adversarial examples with adversarial networks," *arXiv preprint arXiv:1801.02610*, 2018.

[22] H. Huang, R. He, Z. Sun, and T. Tan, "Introvae: Introspective variational autoencoders for photographic image synthesis," in *Advances in Neural Information Processing Systems*, 2018, pp. 52–63.

[23] A. Nguyen, J. Yosinski, and J. Clune, "Deep neural networks are easily fooled: High confidence predictions for unrecognizable images," in *Proceedings of the IEEE Conference on Computer Vision and Pattern Recognition*, 2015, pp. 427–436.

[24] J. Gilmer, L. Metz, F. Faghri, S. S. Schoenholz, M. Raghu, M. Wattenberg, and I. Goodfellow, "Adversarial spheres," *arXiv preprint arXiv:1801.02774*, 2018.

[25] S. M. Moosavi Dezfooli, A. Fawzi, and P. Frossard, "Deepfool: a simple and accurate method to fool deep neural networks," in *IEEE Conference on Computer Vision and Pattern Recognition*, 2016.

[26] A. Kurakin, I. Goodfellow, and S. Bengio, "Adversarial examples in the physical world," *arXiv preprint arXiv:1607.02533*, 2016.

[27] M. Mirza and S. Osindero, "Conditional generative adversarial nets," *Computer Science*, pp. 2672–2680, 2014.

[28] D. P. Kingma, D. J. Rezende, S. Mohamed, and M. Welling, "Semi-supervised learning with deep generative models," in *Advances in Neural Information Processing Systems*, 2014, pp. 0000–0000.

[29] Z. Dai, Z. Yang, F. Yang, W. W. Cohen, and R. R. Salakhutdinov, "Good semi-supervised learning that requires a bad GAN," in *Advances in Neural Information Processing Systems*, 2017, pp. 6513–6523.

[30] G. Lample, N. Zeghidour, N. Usunier, A. Bordes, L. Denoyer *et al.*, "Fader networks: Manipulating images by sliding attributes," in *Advances in Neural Information Processing Systems*, 2017, pp. 5967–5976.

[31] P. Upchurch, J. Gardner, G. Pleiss, R. Pless, N. Snavely, K. Bala, and K. Weinberger, "Deep feature interpolation for image content changes," in *Proceedings of the IEEE Conference on Computer Vision and Pattern Recognition*, 2017, pp. 7064–7073.

[32] F. Schroff, D. Kalenichenko, and J. Philbin, "FaceNet: A unified embedding for face recognition and clustering," in *Computer Vision and Pattern Recognition*, 2015, pp. 815–823.

[33] D. Berthelot, T. Schumm, and L. Metz, "BEGAN: Boundary equilibrium generative adversarial networks," 2017.

[34] D. P. Kingma and J. Ba, "Adam: A method for stochastic optimization," *Computer Science*, 2014.

[35] Y. LéCun, L. Bottou, Y. Bengio, and P. Haffner, "Gradient-based learning applied to document recognition," *Proceedings of the IEEE*, vol. 86, no. 11, pp. 2278–2324, 1998.

[36] Z. Liu, P. Luo, X. Wang, and X. Tang, "Deep learning face attributes in the wild," in *International Conference on Computer Vision*, 2015.

[37] M. Abadi, A. Agarwal, P. Barham, E. Brevdo, Z. Chen, C. Citro, G. S. Corrado, A. Davis, J. Dean, and M. Devin, "Tensorflow: Large-scale machine learning on heterogeneous distributed systems," 2016.

[38] G. B. Huang, M. Ramesh, T. Berg, and E. Learned-Miller, "Labeled faces in the wild: A database for studying face recognition in unconstrained environments," Technical Report 07-49, University of Massachusetts, Amherst, Tech. Rep., 2007.

[39] W. Xu, D. Evans, and Y. Qi, "Feature squeezing: Detecting adversarial examples in deep neural networks," *arXiv preprint arXiv:1704.01155*, 2017.

[40] H. Kannan, I. J. Goodfellow, and A. Kurakin, "Adversarial logit pairing," *arXiv preprint arxiv:1803.06373*, 2018.

[41] Y. LeCun, L. Bottou, Y. Bengio, and P. Haffner, "Gradient-based learning applied to document recognition," *Proceedings of the IEEE*, vol. 86, no. 11, pp. 2278–2324, 1998.

[42] F. Tramer, A. Kurakin, N. Papernot, I. J. Goodfellow, D. Boneh, and P. D. Mcdaniel, "Ensemble adversarial training: Attacks and defenses," *International Conference on Learning Representations*, 2018.